ARID ZONE JOURNAL OF ENGINEERING, TECHNOLOGY & ENVIRONMENT
AZOJETE December 2023. Vol. 19(4):747-758
Published by the Faculty of Engineering, University of Maiduguri, Maiduguri, Nigeria.
Print ISSN: 1596-2490, Electronic ISSN: 2545-5818
www.azojete.com.ng

MAXIMUM POWER POINT TRACKING IN PARTIAL SHADED PHOTOVOLTAIC SYSTEM USING SMELL AGENT OPTIMIZATION ALGORITHM

R. O. Amusat[1], S. Shodiya[2], Y. H. Ngadda[1] and D. I. Malgwi[1]

[1]*Department of Physics, University of Maiduguri, Borno Nigeria*
[2]*Department of Mechanical Engineering, University of Maiduguri, Borno Nigeria*

**Corresponding author's email address: amusatramoni@gmail.com*

ARTICLE INFORMATION

Submitted 27 Aug, 2023
Revised 9 Oct, 2023
Accepted 11 Oct, 2023

Keywords:
PV array
Maximum Power Point Tracking
Partial Shading Conditions and
Booster Converter

ABSTRACT

With partial shading conditions, it is essential to acquire Maximum Power Point at which the Photovoltaic systems (PV) operate effectively despite the variation in the cell temperature and incident angle of sunlight rays on the panels. This study explores the use of a Smell Agent Optimization (SAO) algorithm for Maximum Power Point Tracking (MPPT) in partial shaded PV systems. The proposed MPPT system is composed of a PV model, a DC-DC converter model and a control part. The Smell Agent Algorithm (SAA) was adopted in the control part of the MPPT system to implement the optimization algorithm using four different shading patterns (SPs) and to calculate the optimal switching duty cycle of the DC-DC converter. The effectiveness of the proposed system was verified using simulations in the MATLAB/Simulink environment. The SAO respectively track maximum values for Power, Voltage and Current as 845.8476 W, 211.7308 V, 3.99492 A while the maximum values for Power, Voltage and Current for Perturb and Observe (P and O) are 845.0465 W, 211.6305 V, 3.993028 A respectively during SP1. The results showed that the SAO algorithm has excellent tracking results in terms of convergence speed, accuracy, power extracted stability, and dynamic response in reaching the optimum point.

1.0 Introduction

Solar energy is the pathway to an environmentally friendly future energy. Every single day, the sun generates far greater quantities of energy than we require for our daily activities. This allows researchers to create models that can predict the future prospects of renewable energy (Amusat *et al*., 2020). Using renewable energy (Solar energy) to generate electric power has an advantage over other traditional power source of energy owing to its ability to transform directly into electrical energy using the photovoltaic (PV) solar cells. A photovoltaic system is made of semiconducting materials that convert incident photon into electric energy with its conducting qualities adjusted by changing the type and amount of impurities added to the initial semiconducting substance. Solar cells or photovoltaic cells can be combined together to make panels or modules. Large photovoltaic arrays can be created by grouping panels' together (Amusat *et al*., 2020). A solar panel (with numerous cells connected in series and/or parallel) or a set of panels is commonly referred to as an array (Surya and Babu, 2012).

Many efforts have been made in the field of modeling and simulation of diode-based photovoltaic cells but, tracking of the maximum power point at which solar panel operates effectively, incorporating a shading parameter into the conventional PV-array model that will account for varying degrees of shading across individual cells of a given PV-module are the

major concern (Claude and Nazih, 2015). Maximum Power Point Trackers are devices that maximize the output power of Photovoltaic Systems for different ambient conditions and maintain the operation of PVs at their maximum power points (Derbeli *et al.,* 2021). Many studies on MPPT techniques have been conducted (Claude and Nazih, 2015). The MPPT techniques: The Perturbed and Observation (P and O) and Climbing Hill (H and C) techniques are widely used due to their ease of implementation and low sensor requirements (Attou *et al*., 2014; Parween, 2019; Jiang *et al*., 2017; Srushti and Uttam 2013; Lokanadham and Vijaya, 2012). The incremental conductance algorithms compare PV array incremental and instantaneous conductance which track a PV system's maximum power point and transfer high PV energy to the load (William and Ramesh, 2013; Hsieh *et al*., 2013; Rajaram and Sharma, 2015).

Short circuit current (I_{sc}) and open circuit voltage (V_{oc}) can be used to determine the MPP current (I_{MPP}) and MPP voltage (V_{MPP}) (Hadji et al., 2013; Subudhi and Pradhan, 2012). The main disadvantage of this MPPT is the uncertainty that exists in this tracking approach, as demonstrated by the approximate relationship of Isc to I_{MPP} and Voc to V_{MPP}. Also, most research does not consider the effect of partial shading (PSC) on the PV system when determining the MPPT. Research on PV maximum power point tracking has been conducted in recent years and the effect of partial shading has been considered. Researchers discovered that conventional methods have been very poor in tracking the performance with many of them failing to track the true MPP under partial shading of PV arrays. (Nur and Chee, 2014).

As a result of the shortcomings of traditional MPPT algorithms, many research studies have used artificial intelligence (AI) techniques to address the stated limitations. Such as Fuzzy Logic Controller (FLC) and Neural Network (NN) (Seyedmahmoudiana *et al*., 2016; Ramana and Jena, 2015; Lalam and Kalpana, 2013; Zaki *et al.,* 2012; Younis *et al.,* 2012). The FLC which is based on rational data interpretation can find means of retrieving the maximum power under partially shaded and rapidly varying atmospheric conditions. Even though these techniques are efficient when dealing with the nonlinear characteristic I - V curves, they require a significant amount of computation. FLC, for example, deals with operations such as fuzzification, rule-based storage, inference mechanisms, and defuzzification. The enormous amount of data needed for training is a major constraint for NN. More so, since the operational conditions of the PV system change continuously, MPPT must respond instantaneously to changes in irradiance and temperature. Therefore, low -cost processors cannot be employed in such a system. Their tracking efficiencies are affected by high control circuit complexity and large data processors for training the system.

There are new MPPT algorithms, inspired by nature and biological structure that were developed to track PV array output power. Among these are Particle Swarm Optimization and Grasshopper Optimization algorithms (Sadegh *et al.,* 2022; Mansoor *et al*., 2020; Saxena *et al*., 2018; Saremi *et al*., 2017; Kashif *et al.,* 2012; Miyatake *et al*., 2011; Chen *et al*., 2010). Some bio-inspired optimizations were introduced to tackle the limitations of conventional techniques based on the literature review. But, handling the most extreme environmental changes such as changing irradiance and PSCs, require an improvement in the aspects of computational burden, precision and accuracy of the result, ease and the convergence of the implementation. Therefore, efforts are made nonstop to look for more current algorithms with good performance. The SAO, which has not been exploit in PV is a current introduced meta-heuristic algorithm, recognized for its robust characteristics in tackling different optimization problems mentioned above. In this study, SAO was explored in tracking the maximum power point of the PV system under partial shading conditions.

Corresponding author's e-mail address: amusatramoni@gmail.com

2 Materials and Method

2.1 Materials

The materials used for this study are the Solar panel of model Tala Power Solar Systems TP250MBZ with specification shown in Table 1, booster converter of the specification shown in Table 2, sensors, MPPT controller and four different SPs of solar irradiance at constant cell temperature of 25°C as shown in Figure 3

Table 1. Key specification of Tala Power Solar Systems PV array Model TP250MBZ type Polycrystalline silicon (156mm×156mm)

Model	Tala Power Solar Systems TP250MBZ
Cell type	Polycrystalline silicon
Maximum Power P_{mp} [W]	249
Open Circuit Voltage V_{oc} [V]	36.8
Short Circuit Current I_{sc} [A]	8.83
Maximum Voltage V_{mp} [V]	30
Maximum Current I_{mp} [A]	8.3
Temperature Coefficient of V_{oc} [%/deg. C]	-0.33
Temperature Coefficient of I_{sc} [%/deg. C]	0.063805
Diode ideality factor	0.94812
Diode Saturated Current I_o [A]	1.0132e-^{10}
Shunt Resistance R_{sh} [Ω]	314.7646
Series Resistance R_{sh} [Ω]	0.2914
Light Generated Current I_L [A]	8.8382
Number of Cell N_{cell}	60

Table 2. Specification of the Booster

Symbol	Parameters	Values
L	Inductance	1.1478 X 10^{-3}
C_{in}	Input Capacitance	10 µF
C_o	Output Capacitance	0.467 X 10^{-3}
R	Load Resistance	53 Ω

2.2 Method

Figure 1 is the schematic diagram of the proposed system. An intelligent control technique based on SAO algorithm for MPPT during unexpected changes in atmospheric conditions was used. The algorithm in the system is used to track the maximum operating point of the solar panel. The SAO is a new meta-heuristic algorithm based on the evaporation of smell molecules in the form of gas and the perception capability of a smell agent. The mathematical model of the SAO consists of three modes- Sniffing, trailing and Random modes (Salawudeen *et al.,* 2021). This is used to update the duty cycle a DC – DC converter, there by tracking the global maximum point while updating the position and velocity continuously as shown in Figure 1. This in turn gives a signal to boost the converter that maintains the operating voltage of the maximum operating point irrespective of the solar irradiance and temperature. To evaluate the performance of the algorithms, the proposed SAO-based MPPT method is implemented on a DC-DC boost converter and its performance was compared with that of the P and O algorithm using Matlab Simulink environment.

Corresponding author's e-mail address: amusatramoni@gmail.com

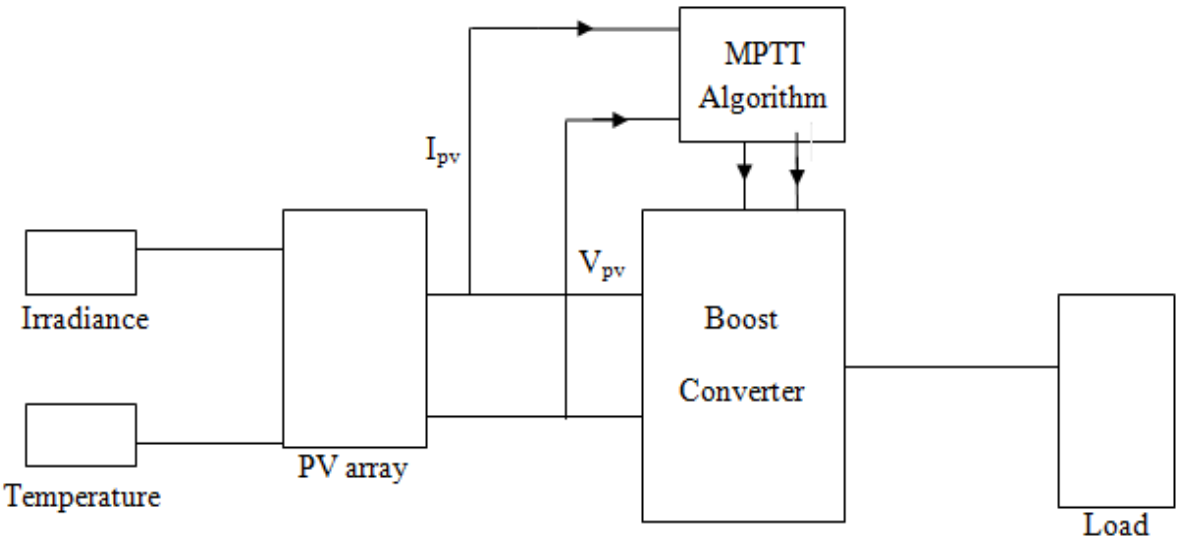

Figure 1: Schematic Diagram of the Proposed PV System (adopted: Attou *et al.,* 2014).

2.2.1 Mathematical Modeling of PV Cell

Photovoltaic cell models have long been a means of describing photovoltaic cell behavior. The most commonly used model for predicting energy production in photovoltaic cell is the single-diode lumped circuit model (Dominique *et al*., 2013). The performance of photovoltaic systems, vis - a-vis, the output current/voltage curve (I-V curve) and Power/Voltage (P-V curve) are studied using an equivalent circuit model. This equivalent circuit consists of a current source with two resistors, one connected in parallel and the other in series. Based on these electronic components, equations (1-5) were used for the photovoltaic systems (Jobeda and Simon, 2018). Figure 2 shows an equivalent circuit of a Photovoltaic with one diode.

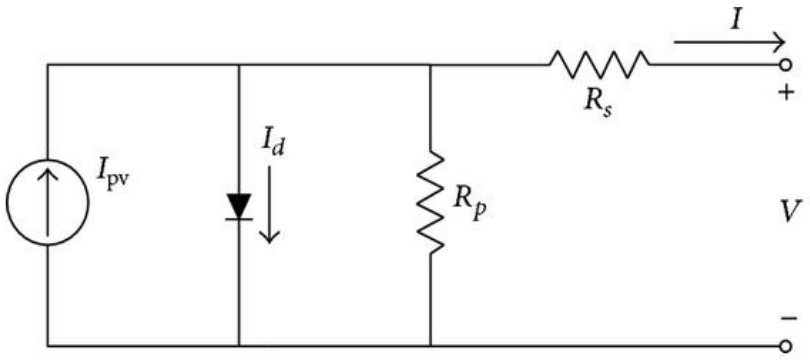

Figure 2: Equivalent Circuit of a Photovoltaic with one diode (adopted: Jieming *et al.,* 2013).

The Mathematical equations of PV from used in the program are shown in equations (1) to (5) (Jobeda and Simon, 2018). The module Ipv (photon current) under the different environmental conditions are related as Eq. (1):

$$I_{pv}(T,S) = \left[I_{sc} + K_i(T_r - T_o) * \left(\frac{S}{1000}\right)\right] \qquad (1)$$

The terms in equation (1) are: K_i is the photon current temperature coefficient; S is solar irradiance (Watt/meter square), T_r is the cell reference temperature in degree (Kelvin), I_{SC} Short-circuit current (Ampere), T_o is the cell operating temperature (Kelvin) which is 25°C at STC

The reverse saturated current at standard testing condition is expressed as Eq. (2):

$$I_{rs} = \frac{I_{sc}}{\left[exp\left(\frac{qV_{oc}}{N_s AKT}\right) - 1\right]} \quad (2)$$

The diode saturated current varies as a cubic function of the temperature and I_o can be expressed as Eq. (3):

$$I_o = I_{rs}\left(\frac{T_o}{T_r}\right)^3 exp\left[\frac{q * E_{go}}{AK}\left(\frac{1}{T_r} - \frac{1}{T_o}\right)\right] \quad (3)$$

In order to assure the parameters required on the consumers, a photovoltaic system has to be made a sufficient number of PV cells interconnected in series or parallel usually called module of array. Then the photon current can be expressed as Eq. (4):

$$\mathrm{I_{pv}} = \mathrm{N_p} * \mathrm{I_{ph}} - \mathrm{N_p} * \mathrm{I_0}\left[\exp\left(\frac{\mathrm{qV_{pv}}}{\mathrm{N_s AKT}}\right) - 1\right] \quad (4)$$

Where $\mathrm{N_p}$ and $\mathrm{N_s}$ are the number of PV cells connected in parallel and series respectively $\mathrm{I_{ph}}$ is Photocurrent (Ampere).

The output power of the PV at any given point as Eq. (5):

$$P = \mathrm{I_{pv}} * \mathrm{V_{pv}} \quad (5)$$

2.2.2 Mathematical Model of the Smell Agent

SAO algorithm is a meta-heuristic algorithm that mimics the process of smell perception (Muhammad *et al.,* 2023; Salawudeen *et al.,* 2021). SAO is classified into 3 modes; these include:

2.2.2.1 Sniffing Mode

The total number of molecules evaporating from the smell source is used in modeling the smell agent algorithm. Each member of the total population is assigned a vector position using Eq. (6) (Salawudeen *et al.,* 2021):

$$X_i^t = [x_{q,1}^t, x_{q,2}^t, ...x_{q,n}^t], \quad (6)$$

where *i*=1,2, 3…, n and q is the population of the smell molecule

A molecule is said to obey Newton's first law of motion (uniform velocity) as it evaporates and moves toward the direction of the smell. The rate of displacement of the smell molecule is denoted by V using Eq. (7):

$$V_i^t = [\mathrm{v}_{q,1}^t, \mathrm{v}_{q,2}^t, ..., \mathrm{v}_{q,n}^t], \quad (7)$$

where *i*=1,2, 3…, n

The equation (7) offers an appropriate velocity for molecule in the proposed SAO.

Since the movement of smell molecules is non-uniform in six-dimensional coordinates, then, velocity is obtained as in Eq. (8):

$$V_{(u.v.w)} = \frac{\Delta X_{(x.y.z)}}{\Delta t} \quad (8)$$

where, $\Delta X_{(x.y.z)}$ is the change in the displacement, x,y,z are the displacement coordinates

Δt is the time interval and $V_{(u.v.w)}$ is the velocity in the u,v,w coordinates.

Using equation (8) the initial position of the smell molecule relative to the Cartesian Coordinate can be represented by Eq. (9):

$$X_{(x,y,z)}^{(t+1)} = V_{(x,y,z)}^{(t)} \ \Delta t + \ X_{(x,y,z)}^{(t)} \tag{9}$$

If Δt = 1 and the iteration increases continuously until all the iterations get exhausted. Then, the initial position of the smell molecule relative to the Cartesian coordinate can be represented as in Eq. (10):

$$X_{(j)}^{(t+1)} = V_{(u,v,w)}^{(t)} \ + \ X_{(x,y,z)}^{(t+1)} \tag{10}$$

As the gas molecule moves in different directions, its velocity can be expressed from the static pressure of the gas as Eq. (11):

$$V = \sqrt{\frac{3KT}{m}} \tag{11}$$

The velocity of the smell molecule from equation (7) is updated as indicated in Eq. (12)

$$V_{(t)}^{(t+1)} = V_{(i)}^{(t)} \ + \ r_o \sqrt{\frac{3KT}{m}} \tag{12}$$

where, $V_{(t)}^{(t+1)}$ is the updated velocity, $V_{(i)}^{(t)}$ is the previous velocity, K is Boltzmann's constant, T is the temperature of the environment of the smell molecules, m is the mass of the molecules and r_o is the random number.

Thus, the updated position of the agent of the smell molecules is given as in Eq. (13):

$$X_t^{(t+1)} = X_i^t + \left(V_{(i)}^{(t)} \ + \ r_o \sqrt{\frac{3KT}{m}} \right) \tag{13}$$

where, $X_{(i)}^{(t)}$ is the previous position of the molecule

2.2.2.2 Trailing mode

This is the movement of the agent continuously toward the region with the highest concentration until the molecule with the overall best is found. This depends on the strength of the olfaction (olf) of the agent (Muhammad *et al.,* 2023; Salawudeen *et al.,* 2018). The movement is done through Eq. (14):

$$X_t^{(t+1)} = X_i^{(t)} + r_1 olf\left(X_{agent}^{(t)} - X_i^{(t)}\right) - r_2 olf\left(X_{worst}^{(t)} - X_i^{(t)}\right) \tag{14}$$

$r_1$andr_2 are random numbers generated at different intervals, $X_{agemt}^{(t)}$and $X_{worst}^{(t)}$ are the fitness of the present position of the agent and the position with the worst smell fitness respectively.

Corresponding author's e-mail address: amusatramoni@gmail.com

2.2.2.3 Random Mode

If there is variation in the intensity of the smell molecule from one point to another over a certain period, the agent may be trapped by local minima resulting in failure in subsequent trailing, then, the agent will execute random mode in searching for the smell molecule source. The random mode is described as in Eq. (15):

$$X_i^{t+1} = X_i^t + r_3 SM \tag{15}$$

where, *SM* is a constant indicating the step movement, and r_3 is a random number that stochastically penalizes the value of the step movement (Muhammad *et al.,* 2023; Salawudeen *et al.,* 2018).

2.2.3 Partial Shading Condition

The PSC has a greater impact on reducing the power generated by solar systems, and this depends upon the shading pattern, the number of bypass diodes, and the solar system arrangement. The partially shaded PV module functions as a load and not as a source of power. This is known as the hot-spot effect, and if the heat produced exceeds a certain threshold, it leads to disintegration and damages the cell, resulting in an open circuit (Al-wesabi *et al.,* 2020).To safeguard against such a hazardous scenario, the bypass diode is installed in the PV system, as shown in Figure 3.The bypass diodes will remain in the reverse cut-off state if the photovoltaic panels are subjected to normal conditions. In the event the PV modules are exposed to the PSC, the bypass diode conducts to form a short circuit; thereby preventing it from getting reversed by the reverse leakage current and enhancing the whole output power. To examine the efficiency of these algorithms, the 4S configuration (Figure 3) was employed in the simulation. This is a well-known configuration for the PV system which consists of four series connected PV modules and has four different power peaks under PSCs. The four different shading patterns (SPs) used in this model correspond to these radiations Pattern 1(1000, 950,900,850 W/m^2), pattern 2 (950,900,850,800 W/m^2), pattern 3 (900,850,800,750 W/m^2) and pattern 4 (850,800,750,700 W/m^2). Each of the four elements of irradiance in each pattern corresponds to the irradiance falling on the PVs.

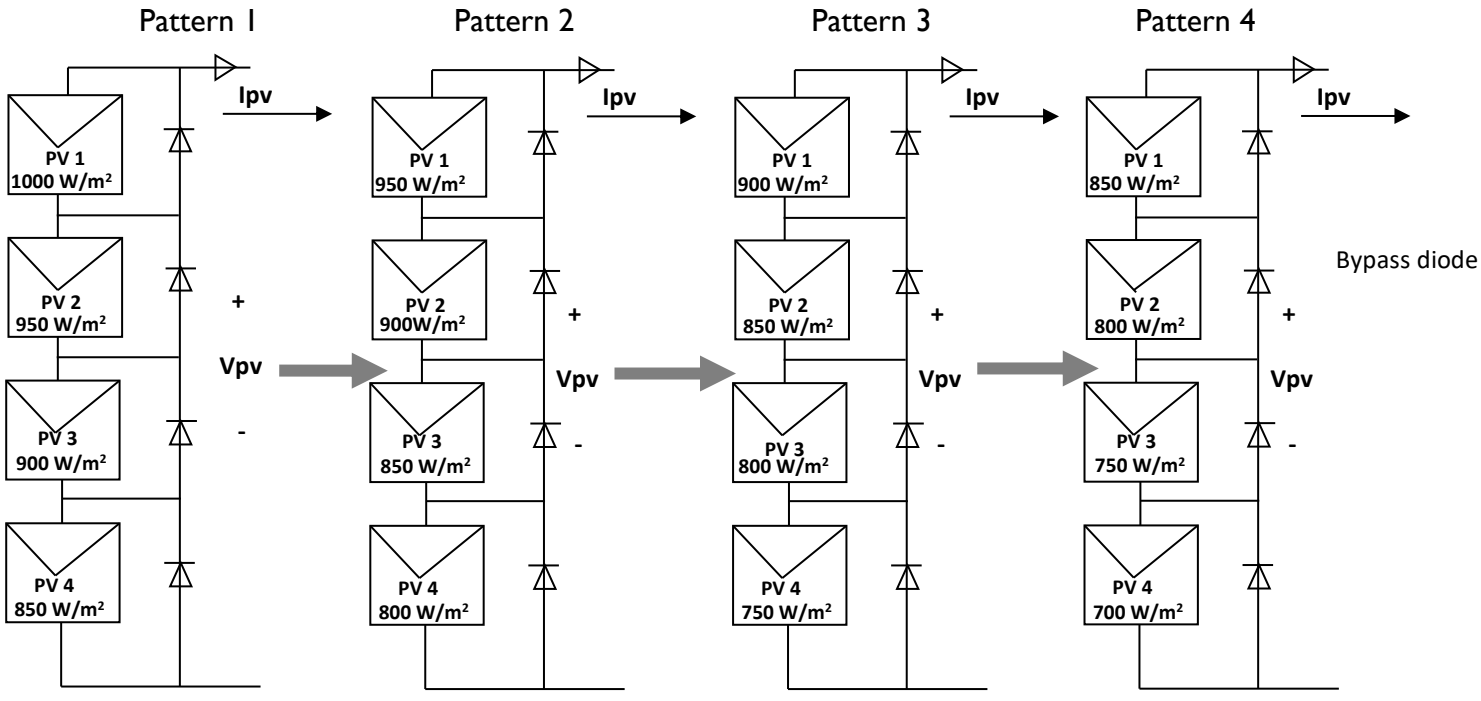

Figure 3: PV Patterns for Partial Shading Conditions (adopted: Sadegh *et al.,*2022)

3. Results and Discussion

The results for the PV system under a temperature of T _ 25 °C and different shading patterns of power for SAO and P and O algorithms are shown in Table 3.These results are for transition from pattern 1 to pattern 4 and consist of several local maximum power points (LMPPs) and only one global maximum power point (GMPP) under PSCs. As shown in Table 4, SAO tracks maximum values for Power as 845.8476 W while the maximum values for P and O as 845.0465 W during SP1. The performance of SAO and P and O algorithms in four patterns have been compared in Table 4which shows that all algorithms succeed in tracking GMPP but the convergence speed of SAO is higher, its efficiency is slightly improved and has less tracking energy losses compared to P and O MPPT algorithms.

Table 3: Shading patterns (SP1, SP2, SP3 and SP4) for Maximum Power of SAO and P and O techniques in Watt (W)

S/N	Pattern 1		Pattern 2		Pattern 3		Pattern 4	
	SAO	P and O	SAO	P and O	SAO	P and O	SAO	P and O
1	0	0	0	0	0	0	0	0
2	688.2668	826.0345	675.2183	772.7223	650.2169	720.7421	593.3545	659.3255
3	628.2921	845.0079	731.9725	794.727	709.6505	744.1879	670.7713	693.1686
4	756.3685	845.0458	764.4782	794.7547	735.3934	744.241	685.2611	693.2556
5	818.0000	845.0452	783.9713	794.7576	741.5228	744.2793	692.9182	693.2257
6	842.2819	845.0456	792.309	794.7556	741.9805	744.244	691.2745	693.2411
7	842.4592	845.0455	792.4423	794.7553	742.1281	744.2403	691.4015	693.2564
8	790.5823	845.0453	776.2829	794.7576	742.6341	744.2794	692.1432	693.2261
9	843.3691	845.0453	793.2386	794.7575	742.7758	744.2463	691.9284	693.2404
10	843.5959	845.0456	793.4373	794.7568	742.9336	744.2439	692.0617	693.2556
11	844.1987	845.0457	793.9608	794.7558	743.3733	744.2789	692.4209	693.2273
12	844.3433	845.0457	794.0848	794.7557	743.4716	744.2441	692.5025	693.2416
13	842.0566	845.0458	793.9811	794.7552	743.6923	744.2435	693.1189	693.2557
14	845.1664	845.0452	794.7898	794.7571	744.0636	744.2436	692.9823	693.226
15	845.5824	845.0452	795.1522	794.7576	744.351	744.2796	693.2221	693.2404
16	845.6837	845.0452	795.242	794.7574	744.418	744.2465	693.2805	693.2544
17	845.7514	845.0452	795.2922	794.7574	744.4675	744.244	693.3165	693.2259
18	845.7999	845.0461	795.3297	794.7555	744.5033	744.2779	693.3434	693.2419
19	845.295	845.0463	795.0421	794.7559	744.5278	744.2446	693.3761	693.2562
20	845.8476	845.0463	795.3871	794.7551	744.5419	744.2419	693.3672	693.2281
21	845.6934	845.0465	794.9709	794.7548	744.5614	744.2765	693.3928	693.2421

Table 4: Comparative Analysis of SAO and P and O Techniques in 4 SP Configuration

Pattern	Target Power (W)	SAO Tracking Power (W)	P and O Tracking Power (W)
1	923.1130	845.8476	845.0465
2	874.3670	795.3871	794.7575
3	825.4070	744.5614	744.2796
4	776.2320	693.3928	693.2564

Figures (4-7) are the detailed simulations of results for the PV system under different shading patterns. The power curves for SAO and P and O algorithms have been shown in Figure (4-7) for a transition from pattern 1 to pattern 4.

Figure 4 shows the power curve for both SAO and P and O corresponding to the partial shading conditions of pattern (1000, 950,900,850 W/m^2), in this case, SAO and P and O respectively track 845.8476 W and 845.0465W as the GMPP and several LMPPs as depicted in Table 3.

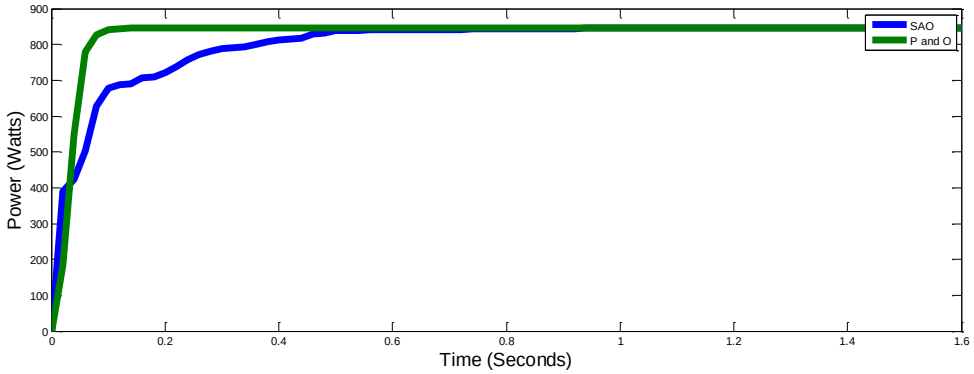

Figure 4: Output Power curve of SAO and P and O models for pattern 1 at 25°C

Figure 5 shows the power curve for both SAO and P and O corresponding to the partial shading conditions of pattern (950,900,850,800) W/m^2. The SAO and P and O respectively track 795.3871 W and 794.7576 W as the GMPP and several LMPPs as depicted in Table 3. The two algorithms track the GMPP but the SAO has a higher value under the same tracking time and partial shading condition as shown in Table 4.

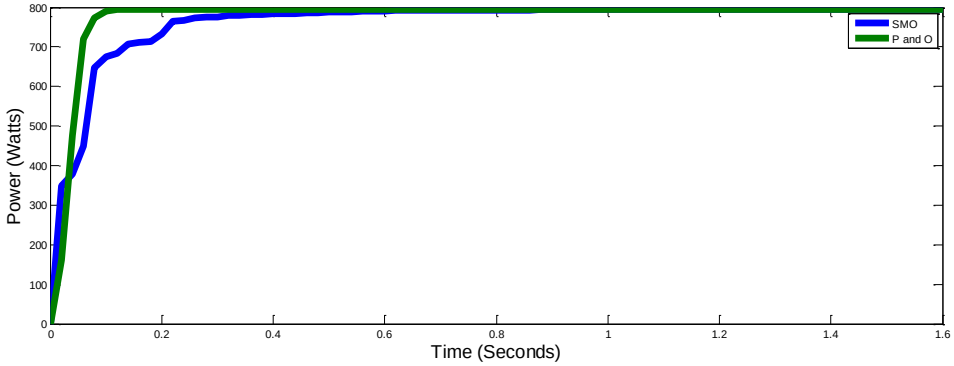

Figure 5: Output Power curve of SAO and P and O models for pattern 2 at 25°C

Figure 6 shows the power curve of the SAO and P and O, this corresponds to the partial shading conditions of the pattern (900,850,800,750 W/m^2). The SAO and P and O respectively track 744.5614 W and 744.2796 W as the GMPP and several LMPPs as depicted in Table 3. In respective of their tracking efficiency. The SAO has a higher value under the same tracking time and partial shading conditions as shown in Table 4

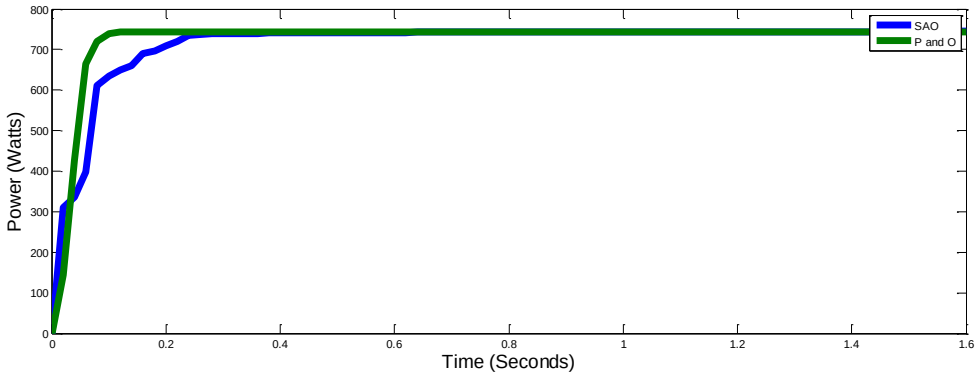

Figure 6: Output Power curve of SAO and P and O models for pattern 3 at 25°C

Figure 7 shows the power curve corresponding to the partial shading conditions of pattern the (850,800,750,700 W/m^2) of both SAO and P and O, in this case, SAO and P and O respectively track 693.3928 W and 693.2564 W as the GMPP and several LMPPs as depicted

in Table 3. Though both algorithms track the GMPP, the SAO has a higher value under the same tracking time and partial shading conditions as shown in Table 4.

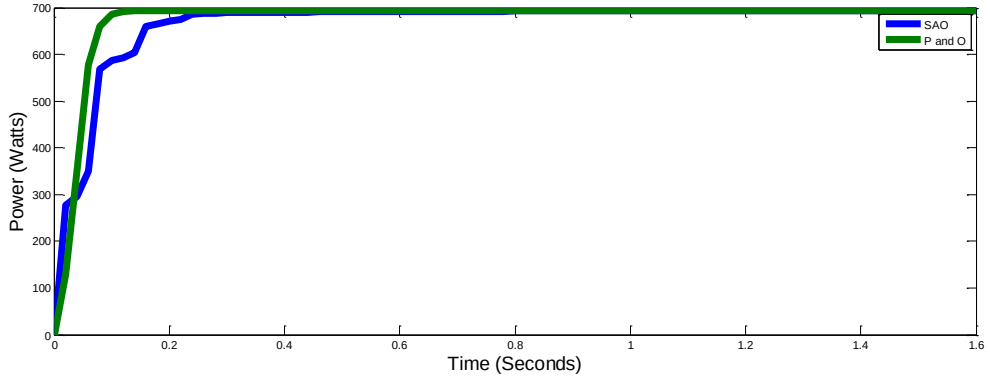

Figure 7: Output Power curve of SAO and P and O models for pattern 4 at 25°C

4. Conclusion

The MPPT based on smell agent optimization was developed using MATLAB/Simulink environment. This was used to track maximum power under partial shading conditions. The Power curves of the shaded PV array have several local peaks and a single maximum power. The effectiveness of the proposed method was determined by comparing its results with conventional techniques (P and O). Both algorithms' responses were observed under various conditions, and the results show that the proposed algorithm has excellent tracking results in terms of convergence speed, accuracy, power extracted stability, and dynamic response in reaching the optimum point.

References

Al-wesabi, I., Shafik, MB., Min, D., Mohammad, AS., Zhijian, F., Ahmed, GA., Tariq, A., Ayman, M. and Al-Rassas. 2020. PV Maximum Power-Point Tracking using Modified Particle Swarm Optimization under Partial Shading Conditions. Chinese Journal of Electrical Engineering, 6(4): 107-121.

Amusat, RO., Shodiya, S. and Ngadda, YH. 2020. Pre- Assessment Model of Solar Photovoltaic Module using User-Friendly Matlab Program. Journal of Science Technology and Education, 8(4): 132-139.

Amusat, RO., Shodiya S. and Ngadda YH. 2020. Mathematical Modeling of Maximum Power of Solar Photovoltaic Systems and Regression Analysis for Field Test Conditions. Nigeria Journal of Engineering Science and Technology Research, 6(1): 104 - 111.

Attou, A., Massoum, A. and Saidi, M. 2014. Photovoltaic Power Control Using MPPT and Boost Converter. Balkan Journal of Electrical & Computer Engineering, 2(1): 23-27

Chen, LR., Tsai, CH., Lin, YL., Lai, YS. 2010. A Biological Swarm Chasing Algorithm for Tracking the PV Maximum Power Point. IEEE Transactions on Energy Conversion, 25: 484–493.

Claude, ZB. and Nazih, M. 2015. A General Review on Photovoltaic, Modeling, Simulation and Economic Study to Build 100 MW Power Plant in Lebanon. British Journal of Applied Science and Technology, 11(2): 1-21.

Derbeli, M., Napole, C., Barambones, O., Sanchez, J., Calvo, I., Fernández-Bustamante, P. Maximum Power Point Tracking Techniques for Photovoltaic Panel: A Review and Experimental Applications. Energies 2021, 14, 7806: 1-31

Dominique, B., Zacharie, K. and Donatien, N. 2013. Modeling and Simulation of Photovoltaic Module Considering Single-Diode Equivalent Circuit Model in MATLAB. International Journal of Emerging Technology and Advanced Engineering, 3(3):493 - 502.

Hadji, S., Gaubert, J. and Krim, F. 2013. Maximum Power Point Tracking (MPPT) for Photovoltaic Systems using Open Circuit Voltage and Short Circuit Current, in 3rd International Conference on Systems and Control,1st October, 2013, Algiers, 87-92.

Hsieh, G., Hsieh, H., Tsai, C. and Wang, C. 2013. Photovoltaic Power-Increment-Aided Incremental-Conductance MPPT with Two-Phased Tracking. IEEE Transactions on Power Electronics, 28: 2895–2911.

Jiang, R., Han, Y. and Zhang, S. 2017. Wide-Range, High-Precision and Low-Complexity MPPT Circuit Based on Perturb and Observe Algorithm. Electronics Letters. 53(16): 1141–1142.

Jobeda, JK. and Simon, YF. 2018. Modeling of a Photovoltaic Array in MATLAB Simulink and Maximum Power Point Tracking using Neural Network. Electrical and Electronic Technology Open Access Journal, 2(2): 40-46.

Kamal, K., Jigar, J., Vishrut, T. and Mitesh, B. 2014. Modelling and Simulation of Photovoltaic Array using Matlab/Simulink. International Journal of Engineering Development and Research, 2(4): 3742-3751.

Kashif, I., Zainal, S., Muhammad, A. and Saad, M. 2012. An Improved Particle Swarm Optimization (PSO)–Based MPPT for PV With Reduced Steady-State Oscillation IEEE Transaction on Power Electronics, 27 (8): 3627–3638.

Lalam, SS. and Kalpana, C. 2013. Artificial Neural Network Implementation for Maximum Power Point Tracking of Optimized Solar Panel. International Journal of Computer Applications, 78 (10): 1-7.

Lokanadham, M. and Vijaya, BK. 2012. Incremental Conductance Based Maximum Power Point Tracking (MPPT) for Photovoltaic System. International Journal of Engineering Research and Applications, 2(2): 1420-1424.

Mansoor, M., Mirza, AF., Ling, Q. and Javed, MY. 2020. Novel Grass Hopper Optimization Based MPPT of PV Systems for Complex Partial Shading Conditions. Solar Energy, 198: 499–518.

Miyatake, M., Veerachary, M., Toriumi, F., Fujii, N. and Ko, H. 2011. Maximum Power Point Tracking of Multiple Photovoltaic Arrays: A PSO Approach. IEEE Transactions on Aerospace and Electronic Systems, 47: 367–380.

Nur, AK. and Chee, WT. 2014. A Comprehensive Review of Maximum Power Point Tracking Algorithms for Photovoltaic Systems. Renewable and Sustainable Energy Reviews, 37: 585-598.

Parween, RK. 2019. Simulation of the Incremental Conductance Algorithm for Maximum Power Point Tracking of Photovoltaic System Based on Matlab. Diyala Journal of Engineering Sciences, 12 (1): 34-43.

Rajaram, CM. and Sharma SK. 2015. Mathematical Modeling of photovoltaic cells using Matlab/Simulink and MPPT Techniques. International Journal of Advanced Research in Electrical, Electronics and Instrumentation Engineering, 4(8): 7170 - 7175.

Corresponding author's e-mail address: amusatramoni@gmail.com

Ramana, V.; Jena, D. 2015. Maximum Power Point Tracking of PV Array under Non-Uniform Irradiance using Artificial Neural Network. In Proceedings of the 2015 IEEE International Conference on Signal Processing, Informatics, Communication and Energy Systems (SPICES),19–21 February, Calicut, India, pp. 1–5.

Sadegh, MT., Mostafa, S. and Kamila, H. 2022. Maximum Power Point Tracking in Partially Shaded Photovoltaic Systems using Grasshopper Optimization Algorithm. IET Renewable Power Generation, 1(1): 1-11.

Salawudeen, AT., Muhammad, BM., Yusuf, AS. and Adewale, EA. 2021. A Novel Smell Agent Optimization: An Extensive CEC Study and Engineering Application. Knowledge Based Systems, 232:1-23.

Salawudeen, AT., Mu'azu, MB., Sha'aban, YA. and Adedokun, EA. 2019. On the Development of a Novel Smell Agent Optimization (SAO) For Optimization Problems. i-manager's Journal on Pattern Recognition, 5 (4): 13-26.

Salawudeen, AT., Mu'azu, MB., Yusuf, AA. and Emmanuel A. 2018. From Smell Phenomenon to Smell Agent Optimization (SAO). A Feasibility Study. Proceedings of ICGET, 79-85

Saremi, S., Mirjalili, S. and Lewis, A. 2017. Grasshopper Optimization Algorithm: Theory and Application. Advance in Engineering. Software 105: 30–47.

Saxena, A., Shekhawat, S. and Kumar, R. 2018. Application and Development of Enhanced Chaotic Grasshopper Optimization Algorithms. Modeling and Simulation in Engineering.2018: 1–14

Seyedmahmoudiana, M., Horan, B., Soon, TK., Rahmani, R., Oo, AMT., Mekhilef, S. and Stojcevskie, A.2016. State of the Art Artificial Intelligence-Based MPPT Techniques for Mitigating Partial Shading effects on PV Systems—A review. Renewable and Sustainable. Energy Review, 64: 435–455.

Srushti, RC. and Uttam, B.V. 2013. Incremental Conductance MPPT Technique for PV System. International Journal of Advanced Research in Electrical, Electronics and Instrumentation Engineering, 2(6): 2719-2726.

Subudhi, B. and Pradhan, R. 2012. A Comparative Study on Maximum Power Point Tracking Techniques for Photovoltaic Power System. IEEE Transactions on Sustainable Energy, 4(1): 89-98.

Surya, JK. and Babu, CS. 2012. Mathematical Modeling and Simulation of Photovoltaic Cell using Matlab-Simulink Environment. International Journal of Electrical and Computer Engineering (IJECE), 2(1); 26-34.

Williamm, IC. and Ramesh, R. 2013. Comparative Study of P&O and InC MPPT Algorithms. American Journal of Engineering Research (AJER), 2(12): 402-408.

Younis, MA., Khatib, T., Najeeb, M. and ARIFFIN, AM. 2012. An Improved Maximum Power Point Tracking Controller for PV Systems using Artificial Neural Network, Przeglad Elektrotechniczny, 88 (3):116-121.

Zaki, AM., Amer, SI. and Mostafa, M. 2012. Maximum Power Point Tracking for PV System using Advanced Neural Networks Technique. International Journal of Emerging Technology and Advanced Engineering, 2(12): 58 -63.

Corresponding author's e-mail address: amusatramoni@gmail.com